Electronic Supplementary Material (ESI) for Analyst.

Supporting Information

Portable and Power-free Serodiagnosis of Chagas Disease using Magnetic Levitating Microbeads

Beatriz Castro, Marina Sala de Medeiros, Behnam Sadri,
and Ramses V. Martinez*

B. Castro
Department of Animal Sciences Purdue
University
270 S. Russell St, West Lafayette, IN 47907, USA

M. Sala de Medeiros, B. Sadri, Prof. R. V. Martinez
School of Industrial Engineering Purdue
University
315 N. Grant Street, West Lafayette, IN 47907, USA

Prof. R. V. Martinez
Weldon School of Biomedical Engineering Purdue
University
206 S. Martin Jischke Drive, West Lafayette, IN 47907, USA

E-mail: rmartinez@purdue.edu

Contents

1 Supporting Materials and Methods

1.1 Test tubes

We fabricated the test tubes from clear polyurethane tubing (OD = 3.2 mm, wall thickness = 0.76 mm, ID = 1.6mm) purchased from McMaster–Carr Inc. (Chicago, IL). The tubing was cut in sections of ~73 mm. We sealed one of the ends of each test tubes using a heat sealing bar (see Figure S1b). Prior to use, the tubes were rinsed and sterilized with ethanol (96%). We used a polyethylene foam to keep the test tubes vertically oriented inside the magnetic levitation stage (Figures 1f, 5a).

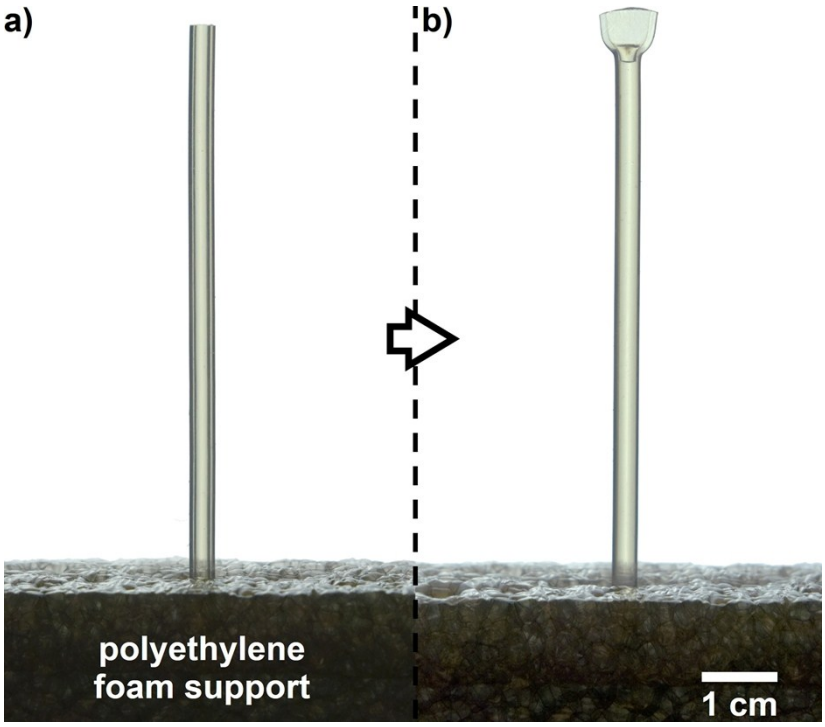

Figure S1. a) Clear polyurethane tubing used in the portable and power-free testing of Chagas disease using MLμBs (OD= 3.2mm, wall thickness= 0.76mm, ID= 1.6mm). b) Test tube after sealing one of its ends.

1.2 Hollow glass beads

We found that hollow glass microbeads commercially available come in a range of densities due to the irregular size of their internal gap. To be able to separate hollow glass beads with high sensitivity using magnetic levitation (with the magnets in a vertical configuration), it is necessary that the density of the beads is close in value to the density of the paramagnetic solution.[1,4] We use Polyamide (Nylon) beads (1 mm in diameter), with a density of 1.15 gcm^{-3} and a magnetic susceptibility $\chi_{Nylon}= -11.5\times10^{-6}$ as a magnetic levitation reference. Once the hollow glass microbeads levitate at their equilibrium positions, we

used a plastic pipette to collect those microbeads levitating at the same height than the Nylon reference bead. Using MLμBs with homogeneous densities in magnetic levitation tests facilitates the visual identification of the presence of beads that levitate at a lower height due to the increase of density caused by the adhesion of T.cruzi antibodies and SiO_2 microcrystals onto their surface.

We calculated the magnetic susceptibility of the glass microbeads using EquationS1:

$$\chi^{ML\mu B} \cong \chi glass \times \frac{V glass}{V ML\mu B} \cong \chi glass \times \frac{\rho glass}{\rho ML\mu B} \quad \text{(S1)}$$

where ρ_{glass} =2.52gcm^{-3}, χ_{glass} =1.39×10^{-5}, $\rho_{ML\mu B}$ =1.15gcm^{-3}, obtaining a value of $\chi_{ML\mu B}$ =3.05×10^{-5}.

1.3 MLμBs

We sonicated the hollow glass microbeads with a narrow density distribution around 1.15gcm^{-3} in ultrapure water for 5 minutes. This step was repeated three times, centrifuging the microbeads at 2000rpm for 3 min in order to deposit the microbeads over the bottom of the vial and being able to change the water with a pipette without significant lost of microbeads. After cleaning, we incubated the microbeads overnight in the antigen solution (iron superoxide dismutase protein excreted, FeSODe of T.cruzi; 110gmL^{-1} in carbonate buffer, pH9.6). We washed the microbeads with PBST (containing a 0.1% of Tween20) and collected them from the bottom of the vial after centrifuging at 2000rpm for 3 min. We repeated the washing cycle three times. To block nonspecific binding of other proteins over the surface of the hollow glass microbeads, we coat them with bovine serum albumin (BSA). BSA coating was performed by adding a 2.5% weight/volume BSA solution in PBS and mixing during 30 min on a shaker. We refer to the hollow glass microbeads coated with T.cruzi antigens and BSA as MLμBs, which were kept in a PBST solution at 4 °C for long term storage.

1.4 Paramagnetic liquid medium

We used a solution of $MnCl_2$ in PBS (1.9 M, result of mixing the incubation layer with the paramagnetic solution at the bottom of the test tube) as the paramagnetic solution used in the magnetic levitation experiments. The solutions were prepared by dissolving $MnCl_2 \cdot 4H_2O$ salt (Alfa Aesar, Ward Hill, MA, 99.5% purity) in PBS (phosphate-buffered saline, Sigma-Aldrich, St. Louis, MO). Since air bubbles can

adhere to the microbeads during the shaking of the test tube, modifying their apparent density, we added to the paramagnetic solution a small concentration of Tween 20 (0.1%, vol/vol) to ameliorate this effect.[1,2] We found that the addition of surfactant to the paramagnetic medium improved the reproducibility of the tests and reduce the time that the MLμBs required to reach their equilibrium position in the magnetic levitation stage. The magnetic susceptibility of the $MnCl_2$ solution at room temperature (T = 296 K) was calculated using Equation S2:[1–3]

$$\chi_{MnCl2} = 1.858 \times 10^{-4} [MnCl_2] - 9 \times 10^{-6} \quad \text{(S1)}$$

where, for a 1.9 M solution of $MnCl_2$, $\chi_{MnCl2} = 3.4 \times 10^{-4}$. Since $\chi_{MnCl2} >> \chi_{MLμB}$, we can assume that small variations in the magnetic susceptibility of the MLμBs did not contribute significantly to the levitation height of the microbeads.

1.5 SiO_2 microcrystals

We used SiO_2 microcrystals (size ~0.5 μm) coated with FeSODe antigens[6–8] to visualize the adhesion of anti-T.cruzi antibodies onto the MLμBs. SiO_2 microcrystals were kept in the paramagnetic medium (bottom layer of the multiphase test tube). SiO_2 microcrystals have a density of 2.65 gcm^{-3}, and sink in the paramagnetic medium, once the test tubes are in vertical position. Once the MLμBs have been incubated in the top layer of the multiphase tube, the tubes are vigorously shaken by hand so that the MLμBs get in contact with the suspension of SiO_2 microcrystals in the paramagnetic medium. The attachment of the SiO_2 microcrystals to the MLμBs partially coated with T.cruzi antibodies, increases the density of the MLμBs, making them levitate at a lower levitation height than those that did not attach to any SiO_2 microcrystal (see Figure 2c,h).

1.6 Multiphase test tubes for POCT using MLμBs

1.6.1 Filling the test tubes:

We used polypropylene plastic dispensing needles (6934A43; McMaster–CarrInc., Chicago, IL) to introduce the 64 μL of MagLev medium (bottom layer) in the test tube first and 6 μL of vegetable oil (middle layer) after. Finally, using also plastic dispensing needles, we deposited 68 μL of the incubating solution—prepared by suspending 20 μg of MLμBs in a 1XPBS solution with a small concentration of Tween 20 (0.1%, vol/vol)—on top of the oil layer, making a three-layer multiphase system (see Figures 1c, S2, S3). We used

disposable pipet tips (CO-RE Tips 50 µL; Hamilton Inc., Reno, NV) to introduce 8 µL of blood/antibody solution in the test tubes (see Figure 1c, S3). Due to the small internal diameter of the test tubes, the oil layer separating the aqueous layers remains stable during the transportation of the tests and enables the mixing of the incubation layer and the magnetic levitation layer after the vigorous shaking of the tube.

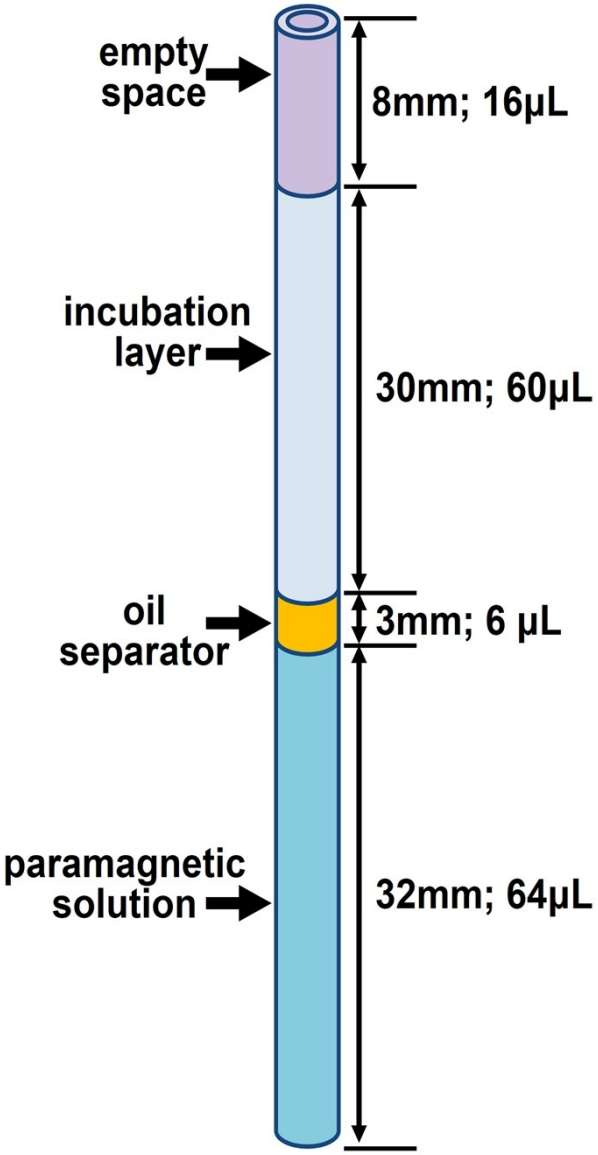

Figure S2. Schematics of the composition of the test tubes used to quantify anti-T.cruzi antibodies in human blood using MLµBs. The clear polyurethane tubes (length = 73 mm, OD = 3.2 mm, wall thickness = 0.76 mm, ID = 1.6 mm) are filled using polypropylene plastic dispensing needles introducing first the paramagnetic solution, then the oil separator, and then the top incubation layer. All the test tubes used in this study had the same composition. To perform the MLµBs tests, we first mix 10µL of blood with 38µL of a PBST solution of antibodies. Then, we introduced 8µL of the blood/antibodies solution on the empty top section of the tube using a plastic dispensing needle.

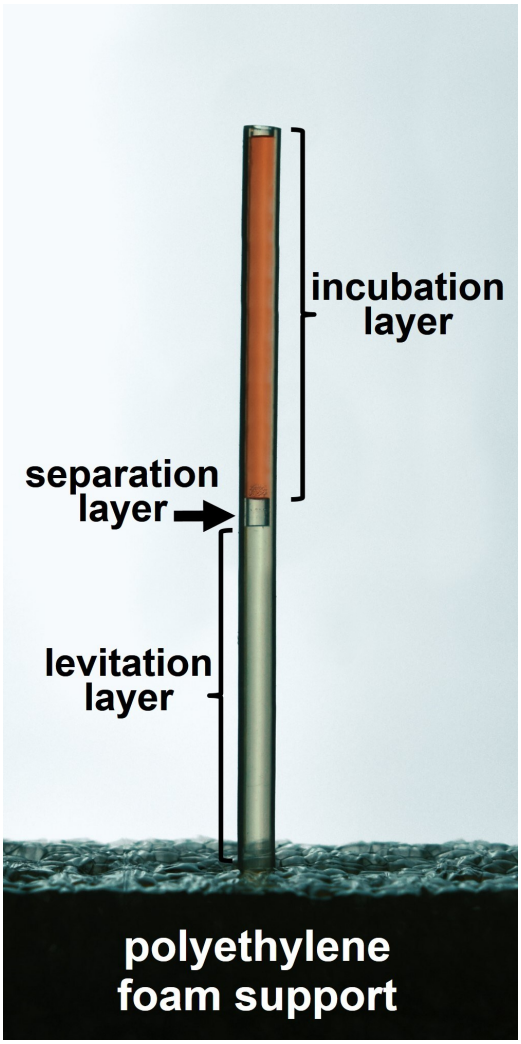

Figure S3. Multiphase test tube used for portable and power-free testing using MLμBs.

1.6.2 Stability of the test tubes

Polyurethane exhibits an apparent static contact angle of ~94 °C with water and ~40 °C with vegetable oil. After filling the bottom of the polyurethane tubing (OD= 3.2mm, wall thickness= 0.76mm, ID= 1.6mm) with 64μL of paramagnetic MagLev medium, we added a thin layer (~6μL) of vegetable oil (middle layer) that wetted the walls of the polyurethane tubing and sealed the paramagnetic medium. After depositing 34μL of the incubating solution as the top layer of the tube, the vegetable oil layer is stable upon small/medium vibration of the test tubes, enabling the transport of the tubes (see Figure S2, S3). Vigorous agitation (by hand), moves the vegetable oil layer and enables the mixing of the aqueous solutions. After the test tube is agitated, the oil droplets accumulate in the top of the test tube due to their lower density.

1.7 Magnetic levitation stage

We used two NdFeB magnets (grade N52, 15 cm × 5 cm × 2.5 cm), purchased from K&J Magnetics Inc. (www.kjmagnetics.com; Pipersville, PA) in our MagLev stage. The high remanence of the NdFeB magnets maintained the magnetization constant during the experiments even with the magnets placed in an anti-aligned configuration. A long screw system approached the top magnet to the bottom one keeping them parallel at all times. We used a bubble level to ensure that the direction of the magnets was parallel to the gravitational vector.

Important safety considerations: During the assemble of the MagLev stage is necessary to be very careful with the handling of the NbFeB magnets. Prior to mounting the magnets on the MagLev stage, we removed all magnetic objects from the proximity of the stage. We placed the magnets in the MagLev stage one at a time, using thick anti-vibration gloves (McMaster–Carr Inc.) and safety glasses. After securing the first magnet in the stage with a screw, we separated it as much as possible from the place where the second magnet would be mounted (40 cm distance) and covered the magnet with several layers of polyethylene foam and adhesive tape to prevent the accidental attachment of the two magnets. The second magnet was mounted—in an antialigned configuration—with one person holding the stage and another person placing the magnet and securing it with a screw so that their north poles face each other. The polarity of the magnets was verified using a small magnet before removing the polyethylene foam. After its assembly, the MagLev stage is very stable, portable, and easy to use.

1.8 Finite element simulation of the magnetic field and magnetic force

We measured the strength of the magnetic field generated by the NdFeB magnets of the magnetic levitation stage using a Gauss meter (Omega, Model HHG191). We used COMSOL® Multiphysics 5.0.a (COMSOL Inc., Burlington, MA) to simulate the three-dimensional magnetic field and magnetic force field inside the magnetic levitation stage using a value of the remnant magnetization of the magnets $B_r = 1.27$ T and a relative permeability $\mu_{relative} = 1.05$.[2,3]

We used the ray optics module of COMSOL® Multiphysics 5.0.a to simulate the partial collimation of the diffuse light crossing the microbeads (see Figure 2d).

2 Step-by-step protocol to use MLμBs for T.cruzi quantification

2.1 Whole blood model

Whole human blood samples were drawn from individuals previously tested negative for Chagas disease using a Human Chagas IgG ELISA Test kit (8100-35, Cortez Diagnostics Inc.) with informed signed consent. An ethical approval was not required for this purpose. No animals were used in this study. We used a push-button safety lancet (McKesson Prevent®, 28G, needle depth penetration: 1.5 mm) to capillary sampling blood from the middle or ring finger. Prior to blood collection, we cleaned the fingertip of the donor using an alcohol wipe. After pricking the fingertip with the safety lancet, the first three drops of blood were removed with cotton and the following drop of blood was collected using a disposable polypropylene tube loaded with a solution of anti-T.cruzi antibodies in PBST. The mixture of a known concentration of anti-T.cruzi antibodies in PBST and whole human blood constitutes the whole blood model used in this study. We transfer the whole blood model for Chagas disease to the top layer of the test tube to initiate the power-free testing of Chagas disease using MLμBs (Figure 1c).

2.2 Incubation of the MLμBs

After transferring a sample of the whole blood model (with a known concentration of anti-T. cruzi antibodies) to the top layer of the test tube (incubation layer), a final concentration of blood in PBST of ~1:50 is used to incubate the MLμBs. After an incubation time of 45 min, the test tube was hold from the top and was shaken vigorously by hand in order to make the MLμBs to pass from the top layer to the aqueous paramagnetic solution. During the shaking process, blood debris, small bubbles, and oil droplets also mixed with the paramagnetic solution. The introduction of the test tubes in the MagLev stage separated blood debris, any remaining bubbles, and oil droplets from the levitating MLμBs in only 9 min.

2.3 Reading of the MLμBs

We used indirect illumination to visually identify the levitation heights of the MLμBs. The spherical glass shell of the MLμBs partially collimates indirect illumination, allowing the user to perceive a set of bright spots projected on a thin and translucent layer of white cellulose paper (Mylifeunit Inc.) in the test tube that facilitate the identification of the position of the levitating MLμBs. To be able to automate the reading process and to couple MLμBs with telemedicine applications, we created a machine-vision algorithm that automatically processes images of the MLμBs taken with a digital camera and facilitating the identification and quantification of anti-T.cruzi antibodies in human whole blood. This algorithm is capable of providing fast diagnostic results to users experiencing difficulties to identify MLμBs by eye. Additionally, the

machine-vision algorithm automatically stores the results of the tests and can transmit them, through the internet, to remote experts, facilitating telemedicine applications.

Figure S4 shows the different image processing steps automated by our algorithm for every digital image received. Briefly, the algorithm applies first a white balance correction filter to improve the contrast of the original image, then the image is transform into black and white using customizable threshold levels.[9] Finally, the contributions of the paper screen and the background are removed from the black and white image and the gaps in L_1 and L_2 are filled to facilitate the automatic quantification of T.cruzi antibodies in blood. The machine-vision algorithm used in this study can be found at the end of the Supporting Information.

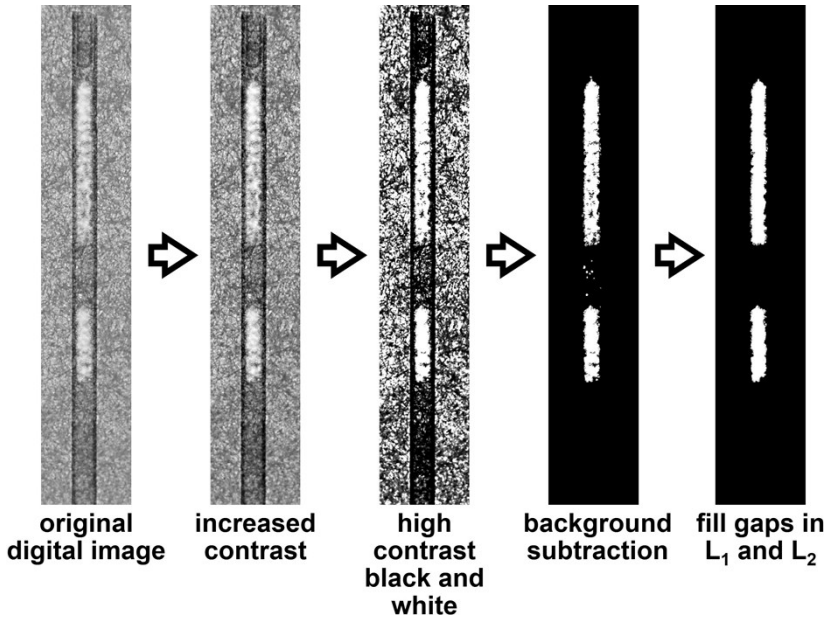

Figure S4. Image processing steps performed by the machine-vision algorithm used for the automatic detection and quantification of anti-T.cruzi antibodies in human blood using MLμBs.

2.3.1 Reducing the reading time of the MLμBs

It is possible to reduce the time required for the MLμBs to reach their levitation height by increasing the strength of the magnetic field in the MagLev stage at the beginning of the test. Figure S5 shows the simplicity of the implementation of this approach: First, before the test tube is inserted at the MagLev stage, the user brings the magnets closer (d∼5cm). When the MLμBs is inserted in the MagLev stage, the beads

respond faster to the magnetic forces induced by the stage (now stronger than when the magnets were more separated). The increased magnetic field makes the microbeads to form a big cluster in the center of the stage (where the field is minimum, see Figure 2a, b) in 1 minute. Then, to regain the resolution of test, the magnets need to be separated to a distance d = 19cm (see Figure 4c). This procedure reduces the testing time to ~6 minutes, preserving the resolution of the technique.

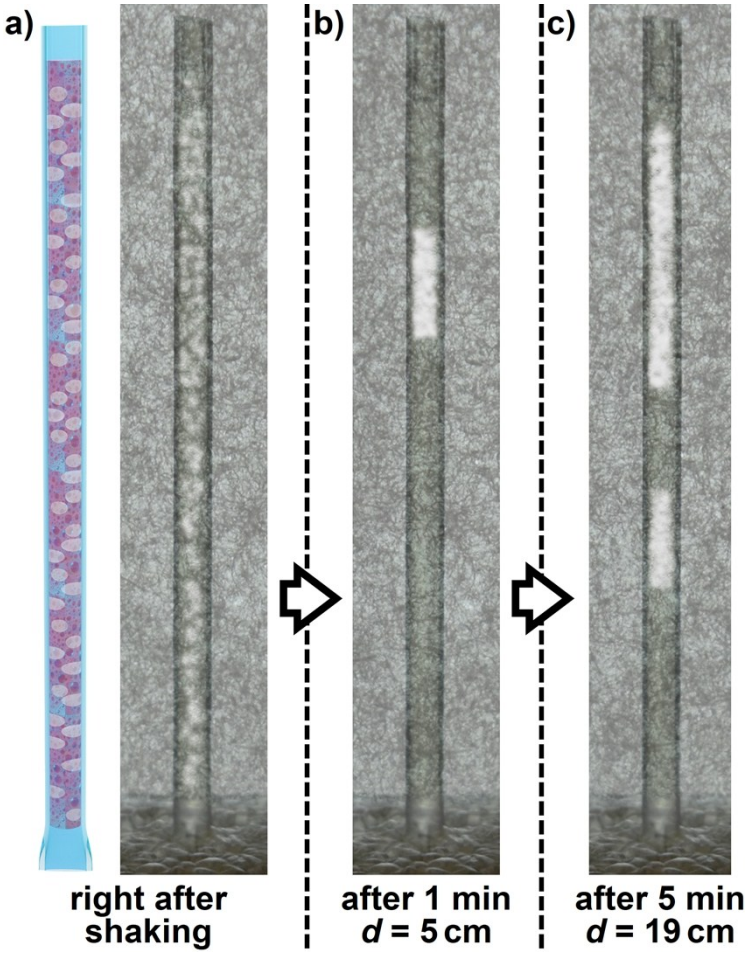

Figure S5. Decreasing the levitation time of the MLμBs by increasing the magnetic field during the first minute of the test (decreasing the distance between the magnets). a) After the tube is shaken to mix the top and bottom aqueous phases, the test tube is inserted in the MagLev (distance between magnets, d = 5 cm). b) After 1 min, the beads form a big cluster in the center of the MagLev stage, where the field is minimum. c) After the first minute, the magnets are separated to d = 19 cm, allowing the MLμBs to get to their levitation heights in 5 min.

3 Accuracy, Sensitivity, and Specificity of MLμBs

The whole blood model tested in this study was prepared by mixing blood tested negative for anti-T.cruzi with a known solution of IgG anti-T.cruzi antibodies in PBST. To elaborate a calibration curve, we measured each of the concentrations using 26 independent experiments (different test tubes) and used the relative standard deviation to evaluate the precision of the tests.[11] We assessed the accuracy of MLμBs by comparing the obtained results with the expected result from the calibration curve, finding a 97.2% of agreement.

We define sensitivity as the percentage of samples correctly identified using MLμBs. During the tests, we found that MLμBs were able to correctly diagnose 100% of the blood samples contaminated with concentrations of T.cruzi as low as 5 μgmL^{-1} (detection limit). In this study, we did not used blood samples infected with other diseases co-endemic with Chagas (such as visceral leishmaniasis) so that, even though we used a specific antigen for T.cruzi identification,[30,31] that have demonstrated in previous studies high sensitivity (99.13%), specificity (96.01%), and immunogenicity for Chagas disease in similar buffered solutions of whole blood,[6–8] we cannot assess the specificity of MLμBs-based Chagas testing on patients infected with other trypanosomes (such as T. evansi, T. rangeli, or Leishmania chagasi).

4 Formulation

The total potential energy density (u_{TOTAL}) of each of the MLμBs levitating in the paramagnetic medium can be calculated using EquationsS3, S4, and S5:[2,3]

$$u_{TOTAL} = \frac{U_{TOTAL}}{V} \tag{S3}$$

$$u_{TOTAL} = u_{magnetic} + u_{gravitational} \tag{S4}$$

$$u_{TOTAL} = -\left(\left(\frac{(\chi_{ML\mu B} - \chi_{MnCl2}) \cdot \vec{B}^2}{2\mu_0}\right) + (\rho_{ML\mu B} - \rho_{MnCl2}) .\vec{g}.\vec{h}\right) \tag{S5}$$

where, U_{TOTAL} is the total energy of each levitating microbead, $\chi_{ML\mu B}$ =3.05×10^{-5} is the magnetic susceptibility of the MLμBs, χ_{MnCl2} = 3.4×10^{-4} is the magnetic susceptibility of the paramagnetic medium, $\rho_{ML\mu B}$ =1.15 gcm^{-3} is the density of the microbeads, ρ_{MnCl2} =1.172 gcm^{-3} for a 1.9 M solution of $MnCl_2$ in

PBST, and, for a vertical alignment of the magnets and the test tubes, the value of the magnetic field vector is $\vec{B}$ = (0,0,B) and the levitation height of the microbead is $\vec{h}$ = (0,0,h).

During their levitation in the MagLev stage, MLμBs will minimize their potential energy, reaching the final equilibrium position when $\frac{U}{h} = 0$, which forces an equilibrium in the forces applied to the MLμBs ($F_{magnetic} + F_{gravitational} = 0$), obtaining Equation S6:

$$h_{equilibrium} = \frac{(\chi_{ML\mu B} - \chi_{MnCl2})}{2g\mu 0 \cdot (\rho_{ML\mu B} - \rho_{MnCl2})}(B \cdot \nabla)B \qquad \text{(S6)}$$

In order to make sure that the simulated values of the magnetic field and force were accurate, we compared the experimentally measured magnetic field along the surface of one of the magnets of the MagLev stage with the simulated field profile (Figure S6).

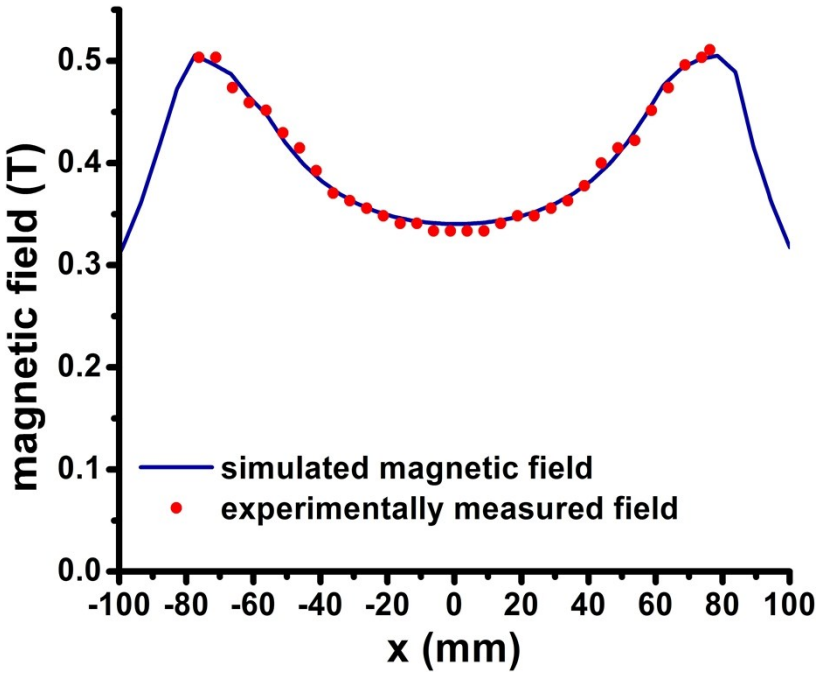

Figure S6. Optimization of the parameters used to simulate the MagLev stage in order to match the magnetic fields measured experimentally. We found that a value of the remnant magnetization of the magnets B_r = 1.27T and a relative permeability $\mu_{relative}$ = 1.05 provided a good agreement between the simulated magnetic field (solid line) and the field experimentally measured on the MagLev stage (dots).

5 Stability of FeSODe in the Paramagnetic Medium

FeSODe of T. cruzi is an antioxidant metalo-enzyme that has demonstrated in previous studies a high stability, sensibility, immunogenicity, and specificity.[6,7] To verify that FeSODe is not adversely affected by the paramagnetic medium used as levitation media ($MnCl_2$), we reproduced the experiments shown in Figure 4 using MLμBs that were kept in $MnCl_2$ for a period of 3h before introducing them in test tubes (see Figure S7 used to run the inmunoassays. After comparing the results of the immunoassays performed with MLμBs previously stored in PBST—medium used for long term storage—and those performed with MLμBs stored for 3h in $MnCl_2$, we see that the relative maximum standard deviation between those measurements is 2.7% (Figure S7). This value of this standard deviation is comparable to the standard deviation of the MLμBs assays to quantify anti-T. cruzi antibodies in whole blood solutions, demonstrating that the paramagnetic medium used as levitation media does not adversely affect the MLμBs.

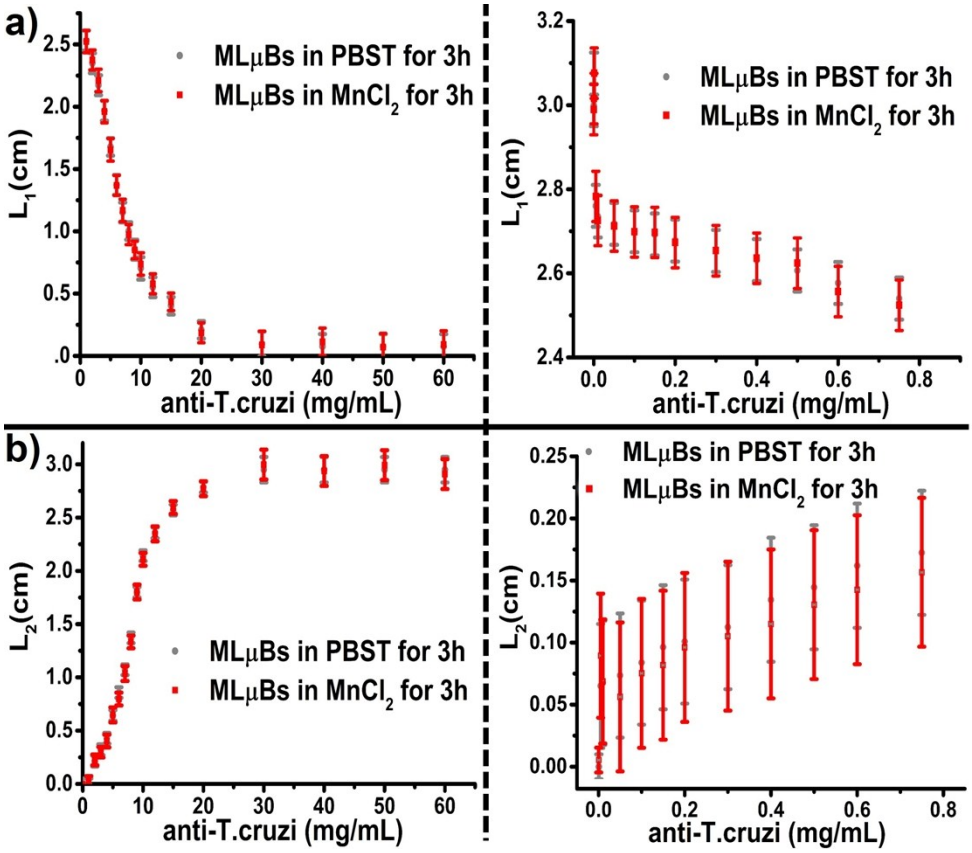

Figure S7. Stability of FeSODe in paramagnetic medium ($MnCl_2{\cdot}4H_2O$ salt dissolved in PBS, 3.8 M; "$MnCl_2$"). Data series in gray corresponds to the results of MLμBs assays obtained using microbeads stored in PBST (buffer solution used in the incubation layer). Data series in red correspond to the results of MLμBs assays obtained using microbeads previously stored in a $MnCl_2$ solution during 3h. The overlap between these data series (standard deviation of 2.7%) indicates that the FeSODe reactivity is not adversely affected by the paramagnetic medium used to levitate the MLμBs.

6 Disposability of MLμBs

We dispose the MLμBs test tubes by incineration.[9,10] When the test tubes are exposed to temperatures greater than 150 °C, the proteins and antibodies in the tube degrade, the hollow glass microbead burst, the aqueous solution evaporates, and the test tube melts generating minimal amounts of residue.

7 Cost of fabrication

We estimate the cost for making each of the test tubes used in the MLμBs assays, without considering labor or capital expenses, to be ~$0.08 each. This total cost, itemized in Table1, is based on costs of small quantities of material and reagents and could be subject to lower prices based on volume discounts. The cost of the safety lancet and the disposable cuvette required to draw blood from the patient are not considered in the calculation of the cost of the MLμBs assays.

Cost per test tube of MLμBs assays	
Hollow glass microbeads	$ 0.041
$MnCl_2 \cdot 4H_2O$ salt	$ 0.0037
Rice paper (reusable screen)	$ 0.0031
Tubing	$ 0.008
Reagents	$ 0.0238
Total cost	**$ 0.0796**

Table 1. Itemized cost of the test tube used to perform one MLμBs assay at the point of care.

The total cost of the MagLev stage we prototyped in aluminum was ~$62 including the magnets. Reducing the cost and weight of the MagLev stage is possible using rigid 3D printed plastic.[1]

8 Matlab Code used for the accurate detection of T.cruzi antibodies in whole blood using MLμBs

We used the following machine-vision algorithm to identify the position of the MLμBs as well as to calculate L_1, L_2, and Z (see Figure 3a). The differences in the illumination of the images can be compensated changing the threshold parameters in the code.[9] The code work in MATLAB® (R2016a) and can be used as a web-based application by running it continuously on a Windows or Ubuntu server. The algorithm, after a digital image is received, identifies the MLμBs after transforming the original image into a high contrast

black and white image (Figure 2f,h and S4). The algorithm automatically stores a dated copy of the original and processed images and transmits the diagnostic results back to the same device that submitted the original digital image, interfacing the MLμBs assays as a telemedicine application.

```
%--------------------------------------------------------------------------
% FlexiLab
% PURDUE UNIVERSITY
%--------------------------------------------------------------------------
%
%
% This program locates the position of the magnetic levitating microbeads % applying
image processing to images of the tests obtained from any digital camera.

% First, import the image captured with the digital camera: captured_image
= imread('MagLevTEST.jpg');

% Find how many rows and columns the captured image has:
n_rows=size(captured_image,1); %number of rows in the captured image
n_columns=size(captured_image,2); %number of columns in the captured image

% Define the CENTER of the captured image: center_row =
round(n_rows/2); %row in the center of the ref image center_column =
round(n_columns/2); %column in the center of the ref image

% Prepare the OUTPUT figure with the microbeads tracked on top and
the % processed image (black and white) on the bottom: figure(1); %
Generates output figure.

if size(captured_image,3)==3 % if the image captured has color, we make it GRAYSCALE
    captured_image=rgb2gray(captured_image);
end

% Prepare the output (2 rows 1 column, we will first define the bottom part of the output) subplot(212)

% Define binary_image as the bottom layer of the final image. Convert image to binary image, based on threshold:
% MODIFY THE THRESHOLD ACCORDING TO THE GLOBAL ILLUMINATION OF THE
captured_image: binary_image=~im2bw(captured_image,0.19);

% We used the bwmorph function to merge the magnetic levitating microbeads into a blurred white area easy to %
distinguish from the black background. Please search "doc bwmorph" to learn more:

% Performs morphological closing (dilation followed by erosion):
binary_image=bwmorph(binary_image,'close');
```

```
% Performs morphological opening (erosion followed by dilation):
binary_image=bwmorph(binary_image,'open');

% Remove small objects (containing fewer than 200 pixels) from the binary image:
binary_image=bwareaopen(binary_image,200);

% Fill image regions and holes. This fills holes in the input binary image. A hole is a set of background %
pixels that cannot be reached by filling in the background from the edge of the image:
binary_image=imfill(binary_image,'holes');

% Displays the image with scaled colors. This function scales the color limits (values of each
% pixel of the image) so that the image uses the full range of the colormap, where the smallest % value in
image maps to the first color in the colormap and the largest value maps to the last color:
imagesc(binary_image);

% Tagging the magnetic levitating beads in the black and white image of the test
L=bwlabel(binary_image); %Generates a matrix L with the connected objects found in binary_image.

% Calculate the areas and other properties of the matrix where all the
% objects are recognized
% Get areas and tracking rectangle properties_tracked_objects=regionprops(L);
% Count the number of objects by counting the number of the same
% properties stored in position 1
N=size(properties_tracked_objects,1);

if N < 1 || isempty(properties_tracked_objects) % Returns if no object in the image.
    nothing_tracked=[ ]; % Define an empty vector
    continue
end

% ---
% Select largest white area in the matrix L, that is the largest number of magnetic levitating %
microbeads we want to track.
areas=[properties_tracked_objects.Area];
[area_max, biggest_object]=max(areas);

% Now we add the top image to the output figure. This image corresponds
% to the original image in grayscale, with a circle tracking the % centroid
of the biggest white area in the L matrix. subplot(211) % Positions the new
image on the top of the output figure.
imagesc(captured_image
); colormap gray hold on

rectangle('Position',properties_tracked_objects(biggest_object).BoundingBox,'EdgeColor',[0 1 1],...
    'Curvature', [1,1],'LineWidth',2.5)

% Finds the center of the largest white area in L (tracked object)
```

```
centerTrackedObject=round(properties_tracked_objects(biggest_object).Centroid);
X=centerTrackedObject(1); % X component of the center of the tracked object.
Y=centerTrackedObject(2); % Y component of the center of the tracked object. plot(X,Y,'c+') %
Adds a nice green cross signaling the position of the center (r = red, c= cyan).

% Superimpose on the image the X and Y coordinates of the center of the tracked object.
text(X+10,Y,['(',num2str(X),',',num2str(Y),',',num2str(frame),')'],'Color',[1 1 1])

% Change the title of the image according to the position of the %
tracked object respect to the center of the image.
if X<center_column && Y<center_row
    title('Majority of L1')
elseif X>center_column && Y<center_row
    title('Majority of L1')
elseif X<center_column && Y>center_row
    title('Majority of L2')
else title('Majority of L2')
end
hold off
drawno
w;
% --

figure(2);
imagesc(captured_image);
%imagesc(cropped_captured_ima
ge); colormap gray hold on
% Finds the center of the largest white area in L (tracked object)
rectangle('Position',properties_tracked_objects(biggest_object).BoundingBox,'EdgeColor',[0 1 1],...
        'Curvature', [1,1],'LineWidth',2.5)
centerTrackedObject=round(properties_tracked_objects(biggest_object).Centroid);
X=centerTrackedObject(1); % X component of the center of the tracked object.
Y=centerTrackedObject(2); % Y component of the center of the tracked object.
%plot(X,Y,'c+') % Adds a nice green cross signaling the position of the center (r = red, c= cyan).

% Superimpose on the image the X and Y coordinates of the center of the tracked object.
%text(X+10,Y,['(',num2str(X),',',num2str(Y),',',num2str(frame),')'],'Color',[1 1 1])

% We get each of the processed images and we save it as a .png in a % folder called "processed_images":
saved_frame = print('-f2', '-noui', '-opengl', '-RGBImage', '-r500'); outputFileName =
sprintf('processed_images/output_image_%d.png',frame); % Generate a name for each output file.
imwrite(saved_frame,outputFileName,'png') % Save the image.


msgbox('Operation Completed','Success'); % Success message when all the frames have been exported.
return; % Exit the program when all the frames have been recorded
```

References

[1] Nemiroski, A., Soh, S.; Kwok, S. W.; Yu, H.D; Whitesides, G. M. *J. Am. Chem. Soc.* **2016**, *138*, 1252–1257.

[2] Atkinson, M. B.; Bwambok, D. K.; Chen, J.; Chopade, P.D.; Thuo, M.M.; Mace, C. R.; Mirica, K. A.; Kumar, A. A.; Myerson, A. S.; Whitesides, G.M. *Angew. Chem. Int. Ed.* **2013**, *52*, 10208–10211.

[3] Mirica, K.A.; Shevkoplyas, S. S.; Phillips, S. T.; Gupta, M.; Whitesides, G. M. *J. Am. Chem. Soc.* **2009**, *131*, 10049–10058.

[4] Penland, N.; Choi, E.; Perla, M.; Park, J.; Kim, D. H. *Nanotechnology* **2017**, *28*, 075103.

[5] Baday, M.; Calamak, S.; Durmus, N. G.; Davis, R. W.; Steinmetz, L.M.; Demirci, U. *Small* **2016**, *12*, 1222–1229.

[6] Concha-Valdez, F.; Marín, C.; Cañas-Ruíz, R.; Sosa-Matú, C.; Escobedo-Ortegón, *J. J. Immunol. Infect. Dis.* **2017**, *4*, 105.

[7] Marín, C.; Longoni, S. S.; Urbano, J.; Minaya, G.; Mateo, H.; Jose, A.; Rosales, M. J.; Pérez-Cordón, G.; Romero, D; Sánchez-Moreno, M. *Am. J. Trop. Med. Hyg.* **2009**, *80*, 55–60.

[8] Valdez, F. C.; Marín, C.; Abuxapqui, J. F.; Ortegón, J. E.; Cañas, R.; Moreno, M. S. *Pediatr. Infect. Dis. J.* **2016**, *35*, 739–743.

[9] Pal A.; Cuellar H. E.; Kuang R; Caurin H. F.; Goswami D.; Martinez R. V. *Adv. Mat. Tech.* **2017**, *2*, 1700130.

[10] Weigl, B. H.; Bardell, R.; Schulte, T.; Battrell, F.; Hayenga, J. *Biomed. Microdevices* **2001**, *3*, 267.

[11] Anderson-Sprecher, R. *Am. Stat.* **1994**, *48*, 113.